Kinetic Diversity of Na^+ Channel Bursts in Frog Skeletal Muscle

JOSEPH B. PATLAK and MAURICIO ORTIZ

From the Department of Physiology and Biophysics, University of Vermont, Burlington, Vermont 05405

ABSTRACT Individual Na^+ channels of dissociated frog skeletal muscle cells at 10°C fail to inactivate in 0.02% of depolarizing pulses, thus producing bursts of openings lasting hundreds of milliseconds. We present here a kinetic analysis of 87 such bursts that were recorded in multi-channel patches at four pulse potentials. We used standard dwell-time histograms as well as fluctuation analysis to analyze the gating kinetics of the bursting channels. Since each burst contained only 75–150 openings, detailed characterization of the kinetics from single bursts was not possible. Nevertheless, at this low kinetic resolution, the open and closed times could be well fitted by single exponentials (or Lorentzians for the power spectra). The best estimates of both the open and closed time constants produced by either technique were much more broadly dispersed then expected from experimental or analytical variability, with values varying by as much as an order of magnitude. Furthermore, the values of the open and closed time constants were not significantly correlated with one another from burst to burst. The bursts thus expressed diverse kinetic behaviors, all of which appear to be manifestations of a single type of Na^+ channel. Although the opening and closing rates were dispersed, their average values were close to those of α_m and $2\beta_m$ derived from fits to the early transient Na^+ currents over the same voltage range. We propose a model in which the channel has both primary states (e.g., open, closed, and inactivated), as well as "modes" that are associated with independent alterations in the rate constants for transition between each of these primary states.

INTRODUCTION

Tetrodotoxin (TTX)-sensitive Na^+ channels cause the rapid, but transient, increase in conductance upon membrane depolarization that gives rise to action potentials in nerve and muscle (Hodgkin and Huxley, 1952; Campbell and Hille, 1976). It has long been assumed that the channel switches through a series of functional "states" as it progresses from its resting to its conducting and finally its inactivated conformations. Most investigators who have sought to model this behavior have also made the simplifying assumption that the population of channels in a given membrane, whose activity sums to yield the macroscopic activity, is made up of independent, functionally identical members (see review by French and Horn, 1983).

Address reprint requests to Dr. Joseph Patlak, Department of Physiology and Biophysics, University of Vermont, Given Building, Burlington, VT 05405.

J. GEN. PHYSIOL. © The Rockefeller University Press · 0022-1295/89/08/279/23 $2.00
Volume 94 August 1989 279–301

Even with the advent of single-channel recording (Neher and Sakmann, 1976), and its application to single Na^+ channel currents (Sigworth and Neher, 1980), this assumption has been difficult to test. Most patches that can be studied have more than one Na^+ channel present, each of which opens but a small number of times after membrane depolarization (Aldrich et al., 1983; Horn and Vandenberg, 1984). Since hundreds of open/closed events are required to characterize a channel's kinetics, the characteristics of an individual Na^+ channel cannot be identified with precision at any given instant. Nevertheless, substantial variability in the optimum kinetic parameters are observed from one patch to the next (e.g., Horn and Vandenberg, 1984). The source of such variability remains an open question.

In addition to the transient Na^+ current after depolarization, a small sustained TTX-sensitive Na^+ current has been seen in many preparations (Reuter, 1968; Attwell et al., 1979; Shoukimas and French, 1980; Carmeliet, 1984, 1987). We became interested in the single-channel basis for this late current as an alternative source of information about single Na^+ channel kinetics (Patlak and Ortiz, 1986), and we discovered that most of the late current was due to the occasional failure of Na^+ channels to inactivate for extended periods during prolonged depolarization. The resulting activity of these noninactivating channels is a "burst" of many openings and closings that can last for hundreds of milliseconds, and that can be attributed to the activity of an individual channel. The gating of the channels during these bursts was very similar to that expected for the activation gating, assuming that inactivation had simply been removed (Patlak and Ortiz, 1986). Such bursts thus provided a unique[1] opportunity to characterize an individual Na^+ channel at a particular moment.

We sought to address the assumption of channel homogeneity by studying variability of single-channel characteristics between different bursts. In an initial study (Patlak et al., 1986) we used a statistical test to demonstrate that significant heterogeneity existed in the open-time distributions of bursts within an individual patch. Since it is known that various subtypes of Na^+ channels can be expressed in developing or denervated skeletal muscle (Sherman and Catterall, 1985; Weiss and Horn, 1986), and in other tissues (Noda et al., 1986), one explanation for our results might have been the coexistance of two or more types of Na^+ channel with permanent structural differences, i.e., "static" heterogeneity. In 20% of bursts, however, the open-time kinetics were also heterogeneous during the burst itself (Patlak et al., 1986). We therefore proposed that the heterogeneity we observed was "dynamic" (due to variability in the properties of individual channel molecules, all of which are, on the average, alike).

Such dynamic heterogeneity of kinetics has been seen in many channel types. Single glutamate channels have been shown to have open/closed kinetics that change

[1] Most other methods of removing Na^+ channel inactivation are also known to alter the fast kinetics of the channel as well. For example, batrachotoxin alters both the fast kinetics and their voltage sensitivity (Keller et al., 1986). *N*-bromoacetamide has little effect on the channel's activation kinetics (Oxford, 1981), but it must be applied from the cytoplasmic side of the membrane, thus requiring patch excision, which itself alters the channel's voltage sensitivity (unpublished observations by the authors). We therefore concluded that the spontaneous bursts, although much more difficult to record, involved the smallest perturbation of the channel's behavior.

with time (Patlak et al., 1979; Kerry et al., 1986): batrachotoxin-treated Na^+ channels suddenly shift their rate constants to new values (Moczydlowski et al., 1984; Weiss et al., 1984) Ca^{2+} channels have several modes (Hess et al., 1984); A-type K^+ channels in sensory neurons of rat also appear to burst occasionally (Shrier and Cooper, 1987); Ca-activated K^+ channels of skeletal muscle show at least four modes of activity (McManus and Magleby, 1988); ACh channels exhibit kinetic heterogeneity (Auerbach and Lingle, 1986), as well as one or more substates of conductance that can be observed directly (Hamill and Sakmann, 1981), or inferred from measurements of the fluctuations of current through open channels (Sigworth, 1985). We sought to characterize the dispersion of open- and closed-time constants for bursting Na^+ channels to characterize modes in which they might potentially function.

This paper presents these open- and closed-time constants for bursting channels at four different membrane potentials. Our results remain consistent with the hypothesis of dynamic heterogeneity for the Na^+ channels of adult frog skeletal muscle. Furthermore, we show that both time constants were broadly dispersed from one channel to the next, yet they had little correlation with one another as they varied. Models of the resulting kinetic diversity would require either a large number of possible kinetic modes of activity, or distributed values of the rates of transition between the main states of the channel. Despite the large variation in the observed values of the transition rates, the average of each time constant, when measured over many channels, was consistent with that expected from the macroscopic gating of the normally inactivating Na^+ current.

METHODS

Experimental Methods

The experimental methods used for the present study were essentially as reported in Patlak and Ortiz (1986). In brief, sartorius muscles from the frog, *Rana pipiens*, were dissected, then treated with collagenase and protease until the tissue was soft enough to remove individual fibers. Single fibers were pulled from the muscle and transferred to the experimental chamber, which contained the intracellular dialysis solution (in millimolar: 95 Cs-aspartate, 3 $MgCl_2$, 5 Na_2ATP, 5 HEPES, 0.1 EGTA, pH 7.4). The fibers were cut into 1–2-mm segments in the dialysis solution to permit exchange of the intracellular ions and to reduce the cell's transmembrane potential to near 0 mV.

Patch electrodes were filled with extracellular saline solution (in millimolar: 100 NaCl, 3 KCl, 0.2 $CaCl_2$, 1 $MgCl_2$, 5 HEPES, 5 glucose, pH 7.4). Gigohm seals were formed on the muscle cell surface using standard techniques (Hamill et al., 1981). After seal formation, patches were polarized to -120 mV, then assayed for the magnitude of the fast Na^+ current in response to brief depolarizations to -20 mV. Since the chance that any channel will burst during a given pulse was ~0.0002, we selected patches with relatively large currents (i.e., large number of channels). Most of our selected patches had between 25 and 100 channels, thus producing a burst every 10–20 min of recording. Our protocols were designed to study these late currents while causing a minimum of slow inactivation. 400-ms depolarizing pulses were given at 0.1 Hz from the holding potential (-120 mV) to test potentials of -50, -40, -30, and -20 mV. The resulting currents were corrected for capacitative transients and leak

currents, filtered at 2 kHz with an 8-pole low-pass Bessel filter, then sampled at 10 kHz with a microcomputer. Hyperpolarizing pulses were averaged, scaled, and then added to the data to correct residual transient and leak currents. All recordings were made at 10°C. Some of the bursts analyzed here were also presented in Patlak and Ortiz (1986), although the majority were from a more recent series of experiments using similar conditions.

Half-Crossing Analysis

The kinetic analyses of the bursts were performed using two different techniques. The first was a standard dwell-time analysis based upon half-amplitude crossing as the criterion for determination of channel opening and closing transitions. Preliminary processing of the raw data included subtraction of averaged blank traces, and in some cases, slight additional digital filtering (to 1.5 kHz), which was necessary to increase the signal-to-noise (i/σ) ratio to above 8. Variance-mean analysis (Patlak, 1988) was used to give an accurate determination of the open-channel current level for each burst, and to check for the presence of subconductance levels. In the bursts studied here, subconductance levels accounted for no more than 5% of the total burst duration. When present, those subconductance levels that were less than the half-amplitude current were counted as closed events, while those greater were assumed to be part of the open state. Open and closed dwell-time histograms were assembled from the data using the additional constraint that an event had to be equal to or longer than a minimum threshold to be counted (Colquhoun and Sigworth, 1983). For the analyses presented here, that minimum was set at 200 μs (two sample points). A simplex algorithm (Caceci and Cacheris, 1984) was used to determine the best relative amplitudes and time constants of one or more exponentials fitted to the dwell-time data using the maximum-likelihood criterion (Colquhoun and Sigworth, 1983). Finally, the best fitting time constants were corrected (Colquhoun and Sigworth, 1983; Blatz and Magleby, 1986) for the events that were missed due to the minimum-duration criterion.

Power Spectrum/Amplitude Histogram Analysis

The second analysis technique was based on the combination of power spectrum and amplitude histogram analysis of individual bursts. These methods were used to obtain the average rates for data in which the i/σ was not sufficient to permit accurate half-crossing analysis. This section describes the methods used to obtain and analyze the power spectra and amplitude histograms. The interpretation of the data thus obtained is given in the Results section.

Power spectral densities during bursts were estimated by averaging Fast Fourier Transforms (FFT) from our digitized data, each of which was made from 512 sequential samples. Use of 50% overlap in the FFTs from neighboring data reduced the statistical variability introduced by the transform itself, and permitted up to 14 spectra to be averaged for a 400-ms burst. Estimates of the background noise were made by averaging roughly twice as many spectra from burst-free traces. The traces from which the background spectra were made also contained the occasional brief openings of channels returning from the inactivated state (termed "background" openings in Patlak and Ortiz, 1986). The kinetic component produced by these openings was also subtracted from the burst spectrum since these events overlapped the burst currents as well. The mean and variance of the power estimates at each frequency were recorded for both the burst and background spectra.

The average difference spectra (burst minus background) were fitted with one or more Lorentzian components using a nonlinear least-squares routine. The data were fitted over the range of 20–2000 Hz (n = 102 frequencies) to minimize the errors introduced by filtering

and aliasing. The best fit was taken to be that which minimized χ^2, which was determined as:

$$\chi^2 = \sum_{f=1}^{n} \frac{(D_f - B_f - S_f)^2}{(\sigma_{Df}^2 + \sigma_{Bf}^2)} \tag{1}$$

where D_f is the estimate of mean power of the channel signal at each frequency, B_f is the mean frequency–dependent power of the background noise, S_f is the predicted power for a given set of parameters, σ_{Df}^2 is the variance of the estimated power for the bursts, and σ_{Bf}^2 is the variance of the background power.

Amplitude histograms were analyzed to determine the open state probability, P_o, during bursts. Histograms of the current amplitudes were assembled from the records by assigning each time point to the appropriate amplitude bin of width 0.02 pA. P_o was determined either by (*a*) counting the fraction of all current amplitudes that were greater than half of the fully open current amplitude, or (*b*) by fitting the amplitude histogram with the sum of two Gaussians, then determining the fractional area of the open-state Gaussian. The two techniques gave results that differed from each other by no more than 1–2%.

Modeling the Macroscopic Current

We fitted the "macroscopic" currents measured at potentials between −60 and 0 mV with the predictions of a standard model of Na^+ channel kinetics (Hodgkin and Huxley, 1952; Horn and Vandenberg, 1984). The model had two closed states, one open, and one inactivated state, arranged as:

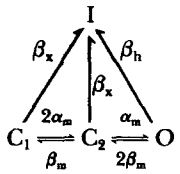

We made the following additional assumptions to constrain our fits: (*a*) the rate constants in the activation pathway are related so as to give m^2 kinetics instead of the m^3 kinetics of Hodgkin-Huxley (1952), since our fast currents were not precise enough to justify the more complex scheme. (*b*) The rates were assumed to follow empirical functions of voltage that had standard form (Adrian et al., 1970, Campbell and Hille, 1976). For the activation/deactivation pathway we used:

$$\alpha_m = \frac{\bar{\alpha}_m \cdot (V_m - \bar{V}_m)}{1 - \exp \dfrac{(\bar{V}_m - V_m)}{V_{\alpha_m}}} \tag{2}$$

$$\beta_m = \bar{\beta}_m \cdot \exp \frac{(\bar{V}_m - V_m)}{V_{\beta_m}} \tag{3}$$

(*c*) The voltage dependence of inactivation from the open state is still controversial. Some investigators support models in which the inactivation rate increases with depolarization (Vandenberg and Horn, 1984), while others support inactivation rate that is voltage independent (Aldrich et al., 1983). Since we currently have no definitive means to discriminate between these two alternatives, we have fitted our transient currents with both models. In model 1, the inactivation rate from the open state, β_h, was assumed to proceed with moderate, saturating, voltage sensitivity, as suggested by Vandenberg and Horn, (1984). Model 2

assumes that β_h had no sensitivity to voltage, as suggested by Aldrich et al. (1983). The inactivation rate from the closed states, β_x, was adjusted to provide the best fits to the mean currents. The inactivation rates could thus be expressed empirically as:

Model 1

$$\beta_h = \frac{\bar{\beta}_h}{1 + \exp\dfrac{(\bar{V}_h - V_m)}{V_{\beta_h}}} \tag{4}$$

$$\beta_x = \bar{\beta}_x \tag{5}$$

Model 2

$$\beta_h = \bar{\beta}_h \tag{6}$$

$$\beta_x = \bar{\beta}_x \cdot \exp\frac{(V_m - \bar{V}_h)}{V_{\beta_x}} \tag{7}$$

To compare the open-state probability curves generated by the model with the currents from a given patch recording we converted the mean current to open-state probability, P_o, using the formula

$$P_o(t) = \frac{\bar{I}(t)}{N \cdot i} \tag{8}$$

where $\bar{I}(t)$ is the time-dependent mean current, i is the single channel current, and N is the number of channels in the patch. Unfortunately, it was not possible to estimate N directly from these data (which were arranged as 43-pulse ensembles), as this requires ensembles of hundreds of pulses at each potential. Instead, we relied on previous measurements in the same preparation in which we measured the peak open probability at −20 mV in 11 long ensembles (>300 pulses) from 8 different patches (Patlak and Ortiz, 1986). This value was found to be 0.4 ± 0.12. We assumed that this estimate was constant from patch to patch. Therefore the number of channels in a patch was determined as

$$N = \frac{\bar{I}_{P20}}{i \cdot (0.4)} \tag{9}$$

where $\bar{I}_{P20}$ is the peak mean current in a given patch at −20 mV. A family of $P_o(t)$ curves could then be generated assuming that this value of N was independent of potential.

Calculation of the open-state probability for models of the fast Na^+ current was performed using either a standard, fourth-order Runge-Kutta algorithm (Press et al., 1986) or the Q-matrix method of Colquhoun and Hawkes (1977), assuming that the left-most closed state was completely occupied at zero time. Fitting of the open probability curves to the data was done by eye. All data analyses were performed on a standard IBM PC/AT (or compatible) computer using Modula-2 (Logitech, Inc., Redwood City, CA).

RESULTS

Open- and Closed-Time Constants of Bursting Channels Are Heterogeneous

Fig. 1 shows seven examples of bursts at −40 mV selected from recordings on six patches to illustrate the diversity of kinetics that we have encountered under essentially identical conditions. For example, the channel bursting in Fig. 1 *A* was open

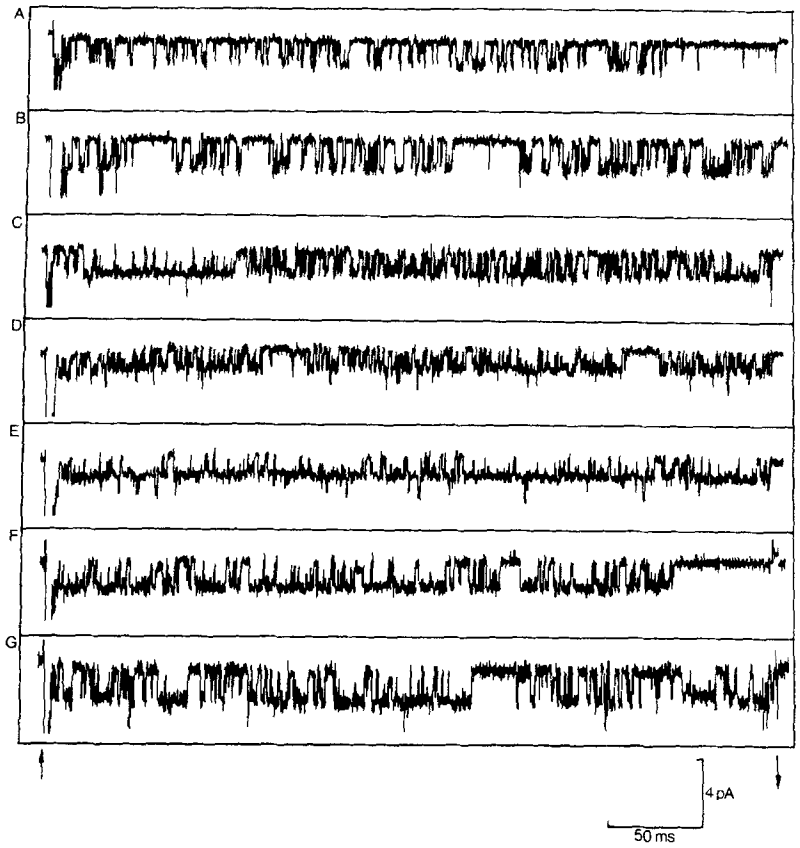

FIGURE 1. Seven examples of long bursts at −40 mV were selected to illustrate the diversity and mutability of their open/closed kinetics. The ON and OFF times of the 400-ms pulses from −120 to −40 mV are indicated by arrows below the bursts. The downward transient of early Na^+ current, due to the simultaneous activity of many tens of Na^+ channels, is truncated at the start of most of the records. Occasional isolated openings of other, nonbursting, Na^+ channels overlap the bursts in some traces. All bursts were recorded at 10°C, and filtered at 2 kHz. $[Na^+]_o$ was 100 mM in *A–E*, 125 mM in *F*, and 175 mM in *G*. The bursts in *D* and *E* were from the same patch. The fractional open times were *A*: 22%, *B*: 33%, *C*: 59%, *D*: 63%, *E*: 89%, *F*: 73%, and *G*: 54% (mean of 56%). Note in particular the sudden changes in kinetics evident in bursts *C*.

22% of the time, while that shown in Fig. 1 *E* was open 89%. Qualitative inspection of these raw data show that both the mean open and the closed times vary from one burst to another. Furthermore, the time constants sometimes changed suddenly during an individual burst (for example Fig. 1 *C*). Although each of these patches contained multiple Na^+ channels, as can be seen by the occasional overlapping "background" events (described in more detail in Patlak and Ortiz, 1986), it is very unlikely that the instances of sudden kinetic alterations were due to the sequential bursting of two different channels. Bursts occurred on the average only once per

50–100 pulses, even in these multiple channel patches. Thus the probability that two bursts would occur in the same pulse without overlapping was minuscule. In contrast, we have shown that 20% of all bursts had significant kinetic inhomogeneity (Patlak et al., 1986).

These bursts at −40 mV have sufficiently large single-channel amplitudes, compared with the level of background noise, to permit a standard kinetic analysis. We used a half-amplitude crossing protocol to assemble histograms of the open and closed dwell times for each burst. We first examined the dwell-time histograms when openings and closings from many different bursts were lumped together to obtain the overall form of their distributions. Fig. 2 shows the lumped open- and closed-time histograms from 30 bursts at −40 mV, with log of the number of events plotted against event duration. Both histograms are roughly exponential in form, but

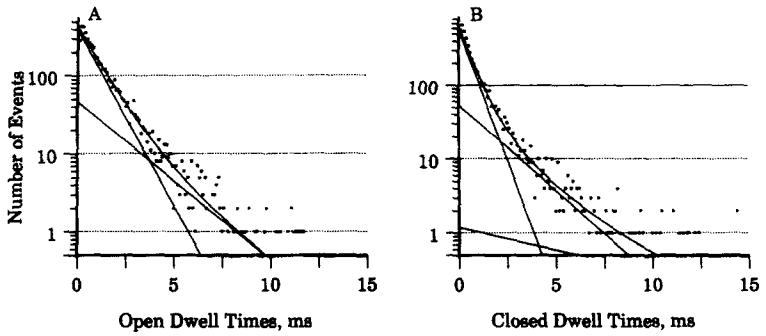

FIGURE 2. Lumped open (*A*) and closed (*B*) dwell-time distributions from 30 different bursts at −40 mV. The histograms were assembled from idealizations of the original data based on the half-amplitude crossing criterion. The number of entries in each bin were added for all the bursts analyzed. Each filled square represents the height of an individual bin of width 0.1 ms. The superimposed curves are the best fitting exponential components (*straight lines*) and their sum (*curved line*) using maximum-likelihood techniques, as described in the text. The open time curve in *A* required two exponentials, with time constants (percent of relative amplitudes) of 0.96 ms (79%) and 2.13 ms (21%). The total number of events was 4,519. The closed-time curve required three exponentials, with time constants of 0.60 ms (77%), 1.82 ms (21%), and 6.56 ms (2%). *N* was 4,343 events.

deviate at the shortest and longest values. The open-time histogram was best fitted by the sum of two exponentials, with time constants (uncorrected for missed events) of 1.0 and 2.2 ms. Addition of a third component gave no significant improvement to the fits using the likelihood ratio test (Rao, 1973; Horn and Lange, 1983). The closed-time histogram was best fitted by three exponentials, with time constants of 0.6, 1.8, and 6.7 ms.

It is not clear, however, that a sum of several exponentials is the appropriate function with which to fit the lumped histograms. If channels can adopt a wide variety of kinetic behaviors when bursting, as we have previously discussed, then the lumped histograms from many bursts might be the sum of a large number of different exponential distributions. The exponentials with which such a histogram is

best fitted probably do not correspond directly to the lifetimes of discrete states of the channel, but are rather those that give an accurate approximation to a much more complex underlying behavior. Kinetic characterization of the channel must therefore be made on the histograms derived from individual bursts.

Fig. 3 shows examples of single-burst histograms, taken from the first three bursts illustrated in Fig. 1. Unfortunately, each burst contained only 75–150 openings, making detailed characterization of all kinetic components impossible. It was not possible to increase significantly the number of events in our histograms for several

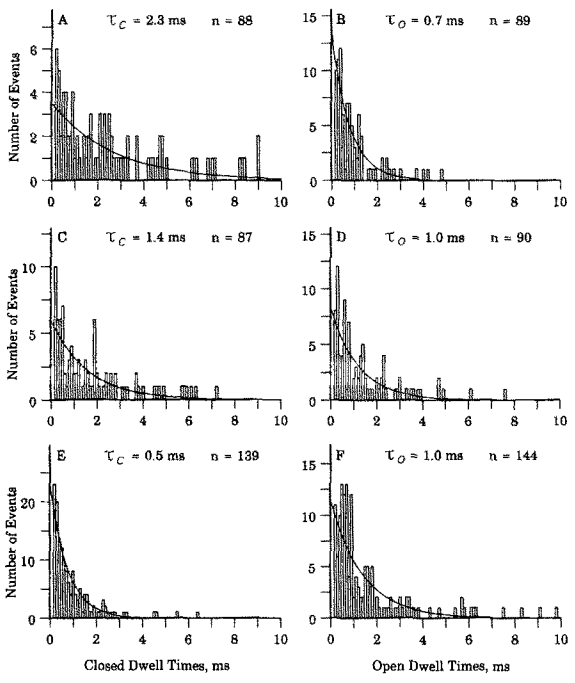

FIGURE 3. Closed and open dwell-time histograms from the first three bursts of Fig. 1. *A* and *B* are from burst *A* of Fig. 1; *C* and *D* are from burst 1 *B*; and *E* and *F* are from burst Fig. 1 *C*. As in Fig. 2, the histograms were assembled using the half-amplitude crossing criterion. Although the idealization coded all half-amplitude crossings in the data, subsequent analysis ignored events that were shorter than 200 μs, combining neighboring events into longer dwell times. This procedure gave a consistent minimum threshold for detection, permitting accurate correction for missed events (see Colquhoun and Sigworth, 1983). The histograms were fitted with a maximum-likelihood algorithm to obtain the best fitting time constant, assuming a single exponential process. The best fitting exponential curve is shown superimposed on each histogram. The value of the time constant, *after* correction for missed events, is shown in each panel. *N* indicates the number of entries in each histogram. The values for *N* were unequal due to elimination of some events near where the traces start and end, and near instances of multiple events.

reasons. First, the length of the bursts appears to be limited by a slow inactivation process, which terminates most bursts within several hundred milliseconds. Second, longer bursts had a greater chance of changing kinetics during the activity, whereas 80–90% of 400-ms bursts were homogeneous. We have therefore limited our analysis to a low resolution examination of the channel's kinetics.

Since the lumped open-time histogram shown in Fig. 2 was nearly as well fitted by a single exponential as by two, this function was used directly for the low resolution fits to the single-burst open-time histograms. The single-burst closed times were

usually also well fitted by a single exponential, but they often had an excess of longer closures, which can also be seen in the raw bursts in Fig. 1. The number of such long events was too low to estimate a slow time constant accurately, even using maximum-likelihood techniques. Instead, we have fitted only events <10 ms in duration to minimize contamination of the fits to the closed-time histograms by these occasional long closures. Each burst in Fig. 3 is shown with the best fitting single exponential under the above constraints. The time constant of this exponential, after correction for missed brief events, is shown in each panel. As expected from the qualitative impressions of the raw data, those time constants are different from one burst to the next.

When such analyses were performed on many such bursts, both the open- and closed-time constants had greater dispersion than would be expected from the variability of the measuring process itself. Fig. 4 *A* shows a log-log plot of the open- vs. the closed-time constants for 21 bursts at −40 mV, recorded with all other conditions as nearly identical as experimentally possible. Open-time constants ranged from 0.23 to 2.0 ms (mean = 1.10 ms, σ = 0.48 ms), while closed-time constants varied between 0.38 and 2.3 ms (mean = 0.80 ms, σ = 0.51 ms). To confirm that this variability was significantly greater than would be expected due to statistical variations inherent in such measurements,[2] we compared it first with that produced when our method of analysis was applied to synthetic data. Fig. 4 *B* shows the result of the half-amplitude crossing analysis when performed on 20 bursts synthesized using a model in which the mean open and closed times were both 1.1 ms. Each burst had 125–150 open or closed events superimposed on background noise and was filtered and sampled to approximate our actual recording conditions. The best fitted time constants, appropriately corrected for missed events, are plotted on the same scale as Fig. 4 *A* (mean open-time constant = 1.04 ms, σ = 0.09 ms; mean closed-time constant = 1.06 ms, σ = 0.14 ms). The variability of these estimates is clearly much less than that of the actual data. Data were also simulated with an additional component of long closures designed to duplicate that which we saw in our recordings. The open- and closed-time constants from such data were similarly distributed, indicating that a poorly resolved slow component cannot have been responsible for the dispersion of the measured values.

Since synthesized data may not realistically approximate the complex processes that underlie Na^+ channel gating, we also sought an alternative method to check our analysis. One instance, in which a channel continued to burst for 12 consecutive pulses during one of our recordings, offered such an opportunity. These bursts appeared qualitatively similar in their kinetics throughout the period of activity. If this channel underwent no changes in its kinetics during these pulses, then its activity could be used to estimate the variability of the measurement technique when applied to actual data. If the channel's kinetics did, in fact, change, then the measurements would nevertheless give an upper bound for the variability. The best fitting time constants for these 12 bursts, each of which had roughly 150 openings/

[2] The expected variability in the time constant produced by fitting 100 events drawn at random from an exponential distribution is approximately σ = 10%. Other errors, such as those introduced by idealizing the data using the half-crossing criterion, and correcting for missed events might add further to this variability.

closings, are shown plotted in Fig. 4 *C*. Although these values have a variability somewhat greater than that of the synthetic data, it was still much less that that of the whole set of bursts. The variability in kinetics that we observe was therefore not due to the limitations of our kinetic analysis.

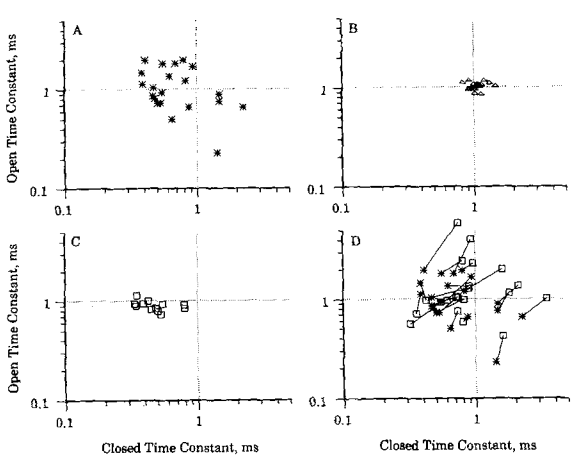

FIGURE 4. Time constants from fits to many bursts in the same conditions. The best fitting open- and closed-time constants (corrected for missed events) for each burst are plotted against one another in each panel. (*A*) The time constants obtained from 21 bursts recorded at −40 mV. Most of these bursts were from different patches, and include the values shown in Fig. 2. In instances where two bursts were recorded in the same patch, they were separated in time by several minutes, and probably were produced by different channels. (*B*) Histogram analysis of bursts synthesized by a two-state model with mean open and closed times of 1.1 ms, i/σ of 8, and with the same overall duration, sample rate, and filtering as the actual data. The results indicate the degree of scatter that is expected from random variability in the expressed kinetics and from the analysis procedure. (*C*) The analysis of 12 sequential bursts recorded in one patch. These bursts were most likely due to the activity of a single channel, since the activity before and after the sequence of bursts was very low. Although it is not known with certainty whether this channel remained homogeneous throughout the recording, no examples of strong shifts in the kinetics (like that shown in Fig. 1 *C*) were observed during the activity. The data give an upper bound for the variability caused by the analysis when applied to actual data. (*D*) Comparison of the time constants produced by histogram analysis and by power spectral/amplitude histogram analysis. The stars are the same data points as shown in *A*. The squares are the time constants (inverse rates) produced by spectral analysis of the same 21 bursts. The two estimates for each burst are connected by a straight line. The values obtained by spectral analysis are, on average, somewhat longer than those of histogram analysis, and have more scatter. Nevertheless, the estimates produced by spectral analysis are usually quite close to those of dwell-time analysis.

Spectral Analysis Shows Heterogeneity at All Test Potentials

The half-amplitude crossing technique was not appropriate to use for the analysis of our data over the full range of potentials that we studied. For bursts at potentials more depolarized than −40 mV, the data required substantial additional filtration to obtain signal-to-noise (i/σ) ratios above 7–8. At the same time, the closed-time kinetics were becoming more rapid. This combination of decreasing channel amplitude and decreasing time constant led to substantial numbers of missed events, and therefore difficulty in the correction of the time constants. Reduction of the i/σ to

values below 7–8, on the other hand, gave significant numbers of erroneous crossings of the half-amplitude threshold, which biased both the histograms and the corrections of the time constants for missed events. We therefore sought an alternative method that could be used to estimate the kinetics of bursting channels with limited i/σ ratios. The technique that we chose was a combination of power spectral analysis and amplitude histogram estimates of the channel's open-state probability.

The power spectra expected for channels that function according to various kinetic models have been discussed in depth elsewhere (Conti and Wanke, 1975; Colquhoun and Hawkes, 1977; Neher and Stevens, 1977). In general, the form of the spectrum is the sum of Lorentzian components, each of which has the form:

$$S(f) = \frac{S_0}{1 + \left(\frac{f}{f_c}\right)^2} \tag{10}$$

Where $S(f)$ is the power at each frequency, f; S_0 is the extrapolated power at 0 Hz (DC component); and f_c is the characteristic (or corner) frequency of the process.

A channel with two states, one open with a constant conductance and the other closed which functions according to the rules of linear kinetics (also called Markovian kinetics), can be described by a single Lorentzian, with:

$$S_0 = \frac{4i^2\alpha\beta}{(\alpha + \beta)^3} \tag{11}$$

and

$$f_c = \frac{(\alpha + \beta)}{2\pi} \tag{12}$$

where i is the single-channel current, α is the opening rate, and β is the closing rate. The spectrum resulting from such a channel can be fitted to obtain estimates of S_0 and f_c.

P_o was determined from amplitude histograms of the bursting currents as described in the methods. For a two-state channel, P_o is a function of the opening and closing rates, with

$$P_o = \frac{\alpha}{(\alpha + \beta)} \tag{13}$$

For a two-state channel, therefore, the forward and backward rates can be estimated by combining the two types of measurements as:

$$\alpha = 2\pi P_o f_c \tag{14}$$

$$\beta = 2\pi f_c - \alpha \tag{15}$$

where f_c is taken from the power spectrum fit and P_o from the histogram fit. The closed-time constant of such a channel, τ_c, is therefore $1/\alpha$, and the open-time constant, τ_o, $1/\beta$.

The accuracy of all fitting techniques, as well as of the combination of the two forms of analysis to solve for individual rates were checked extensively on simulated data at various i/σ ratios. The technique accurately estimated individual rate con-

stants over a wide range of values, and it remained accurate down to i/σ values as low as 2 (when P_o was determined by fitting Gaussians to the amplitude histogram). The variability of the estimates was only slightly greater than that of half-crossing analysis when applied to the same data. This technique appears to be a reasonable way of measuring the kinetics of noisy data. Fluctuation analysis is, however, less sensitive to extra components than dwell-time analysis (Patlak, 1984). Since our

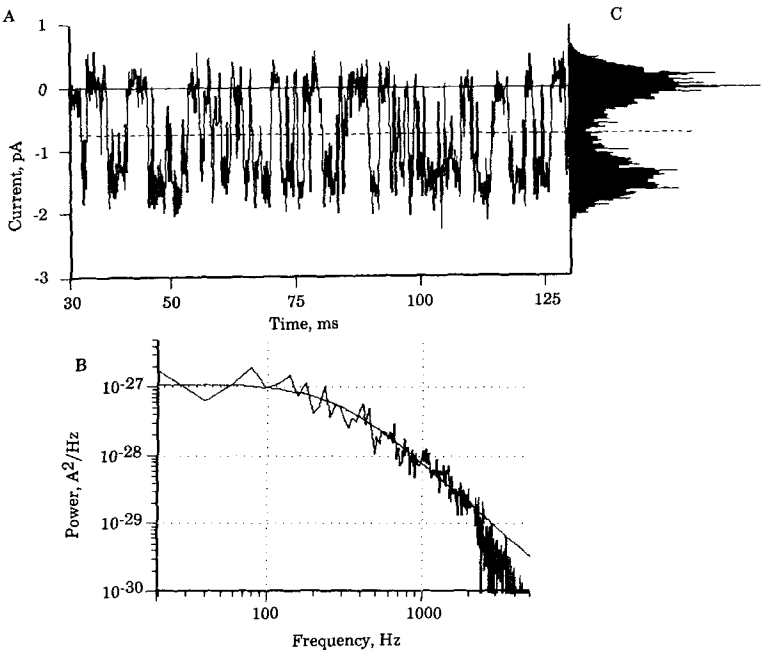

FIGURE 5. Power spectrum/amplitude histogram technique applied to a burst of Na^+ channel openings. (*A*) A 100-ms segment of the burst at −40 mV (filtered at 2 kHz) is shown with superimposed amplitude and time scale. The horizontal line is the average level of the baseline. (*B*) The spectrum that resulted when the 13 power spectra derived from the burst shown in *A* were averaged. The average of 26 estimates of background noise (from two adjacent pulses where no channel was bursting) has been subtracted. The smooth curve is the single Lorentzian that best fit the data between 20 and 2,000 Hz. Addition of a second Lorentzian did not significantly improve this fit. The cut-off frequency, f_c, was 273 Hz. (*C*) The amplitude histogram from the burst in *A*, shown on the same current scale. The dotted line indicates the current amplitude that is equal to half of the fully open amplitude (1.5 pA). P_o was determined as the fraction of histogram entries >0.75 pA, which in this case was 46%. Solving for P_o and f_c gave a forward rate of 789 s^{-1} and a backward rate of 926 s^{-1}.

dwell-time analysis was not able to distinguish multiple exponentials in the data from a single burst, our spectral analysis was similarly limited. As with our dwell-time histograms, we regard these analyses as a low resolution approximation to the potentially more complicated underlying kinetics.

Fig. 5 illustrates the power spectrum/amplitude histogram analysis of a burst at −40 mV (a portion of which is shown in Fig. 5 *A*). The power spectrum from this

burst is shown in Fig. 5 *B*, with the best fitting single Lorentzian curve superimposed. The cut-off frequency (f_c) of this Lorentzian was, in this case, 273 Hz. The fit to the power spectrum was not improved significantly (using an *f* test, Bevington, 1969) by adding a second Lorentzian component. Fig. 5 *C* shows the amplitude histogram during the same burst, with a dotted line superimposed to indicate half of the fully open amplitude. The fraction of entries greater than this level was used to estimate P_o of the channel, which was 46% in this case. P_o and f_c were used as above to estimate the opening and closing rates for the channel, assuming that the underlying kinetics could be approximated as a two-state kinetic scheme. The closed-time constant of this burst was calculated to be 1.3 ms, and the open-time constant was 1.1 ms.

In approximately one-third of the spectra, inclusion of a second Lorentzian component with cut-off frequency below 100 Hz improved the fits to the spectra. This slow component appeared to have been due to occasional long closures that occurred in some bursts, as were also seen in the half-crossing analyses. When necessary, we fitted the spectra with the sum of two Lorentzians to provide a more accurate estimate of the faster, burst-related kinetics. Estimates of the P_o were made in burst segments that were free of such longer events. In simulations of bursting channels that included such occasional long closures, no more than a 10% bias in the estimates of the fast kinetic parameters was found.

To check further the accuracy of the power spectral analysis technique, we used it to measure the kinetics of the same bursts that were analyzed using the half-amplitude crossing technique. The results are shown in Fig. 4 *D*, in which the stars represent the estimates derived from open/closed histograms (the same values as are shown in Fig. 4 *A*), and the squares represent those derived using power spectrum/amplitude histogram analysis. The pairs of estimates produced from a single burst are connected by straight lines. Fig. 4 *D* shows that the power spectral analysis also gave reasonably accurate measurements of the kinetic parameters for our actual data, although there was a tendency toward somewhat longer estimates of the time constants, and for greater variability between estimates. Although power spectral analysis is neither as accurate nor as sensitive as direct measurement of the open and closed times, it does provide acceptable estimates in cases where the background noise is too large to permit half-crossing analysis.

We have used this method to analyze 87 long bursts at four test potentials (12 at −50 mV, 37 at −40 mV, 12 at −30 mV, and 26 at −20 mV). Fig. 6, *A–D* shows plots of open- vs. closed-time constants for the bursts studied at each potential. The resulting kinetic estimates showed that both the open- and closed-time constants were variable at all membrane potentials. Furthermore, no significant correlation could be seen between the values of the time constants (i.e., the estimates were isotropically dispersed in the plots, not colinear). This lack of correlation can also be seen in the estimates of open- and closed-time constants that were derived from half-crossing analysis (shown in Fig. 4 *A*), indicating that this result is also independent of the technique used to measure the kinetics. The lack of correlation between the rates is significant in interpreting the possible mechanisms that might give rise to kinetic heterogeneity.

Average Opening and Closing Rates are Similar to Those of Early Currents

We have speculated previously (Patlak and Ortiz, 1986) that the gating during bursting Na^+ channel currents is controlled by the activation gates of the channel, and that the primary change from the standard, nonbursting mode of the channel is that the inactivation mechanism is inhibited. If this is the case, then the opening and closing rates measured during bursts should be similar to the activation/deactivation rates that would be used to model the macroscopic currents produced by large numbers of channels. Clearly, no estimate of rates from a single member of a heter-

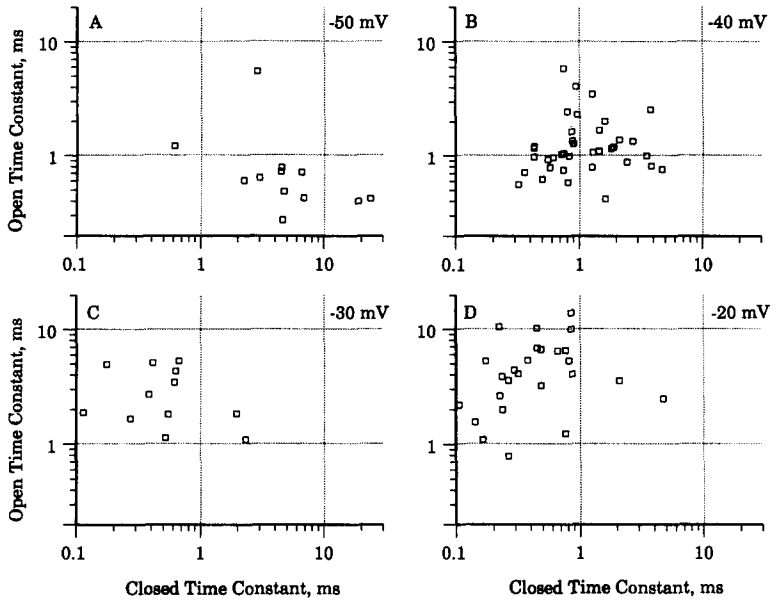

FIGURE 6. The results of power spectrum/amplitude histogram analysis of bursts are shown at four membrane potentials. Each open square plots the open-time constant (inverse of the calculated closing rate) against the closed-time constant (inverse of the calculated opening rate) for one burst. (*A*) Time constants of 12 bursts recorded at −50 mV. (*B*) Time constants of 37 bursts at −40 mV. (*C*) Time constants of 12 bursts at −30 mV. (*D*) The results from 26 bursts at −20 mV. The degree of variability is much greater than expected from the analysis technique alone (not shown, but similar to that shown in Fig. 3 *B* and *C*). The time constants were not significantly correlated at any of the membrane potentials.

ogeneous population of channels can accurately predict the average behavior of all the channels. Nevertheless, the average of the rates measured during many bursts should be comparable to the average behavior of the population, as measured by fits to the macroscopic current.

To make such a comparison, we have made estimates of the activation/deactivation rates by fitting the averaged early currents with a common model of Na^+ channel kinetics. The model that we used, as well as the formula that predicted the volt-

age dependence of individual rate constants, were given in the Methods section. Fig. 7 *A* shows the mean currents from one patch, converted to open probability, with the superimposed predicted probabilities, given by two alternative sets of rate parameters, which are shown graphically in Fig. 7, *B* and *C*. The parameters used to obtain these fits are shown in Table I. Both the opening rate, α_m, and the closing (deactivating) rate, β_m, are the same for the two models.

Although these models, with their fitted parameters, are by no means unique, the fits to the $P(t)$ curves were quite sensitive to the values for both α_m and β_m. Moreover, our estimates of the absolute magnitudes and voltage dependence of α_m and

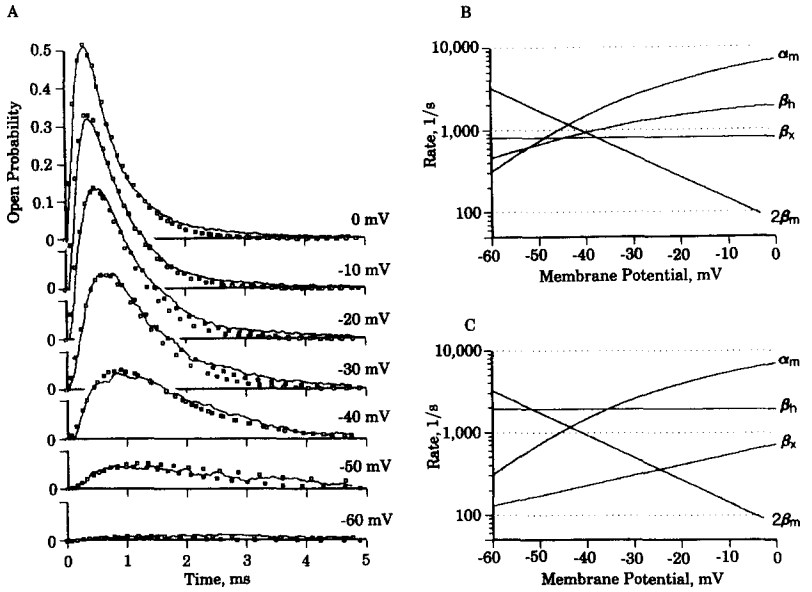

FIGURE 7. Kinetic modeling of the transient Na^+ current from a patch of muscle membrane. (*A*) Open probability curves derived from mean current recordings at the pulse potentials shown next to each trace. The current responses to 44 identical pulses to each voltage were filtered at 5 kHz, sampled at 30 kHz, and averaged. The currents were then scaled by the estimated number of channels, and the single-channel current at each potential (see Methods in test) to give the final open probability estimates. The filled squares are the open probabilities predicted by the model described in the text using the rate constants shown in *B*. The open squares used the rates shown in *C*.

β_m were similar to the independent estimates of other investigators (Hodgkin and Huxley, 1952; Campbell and Hille, 1976; Horn and Vandenberg, 1984; Vandenberg and Horn, 1984; Keller et al., 1986), indicating further that the kinetics used to describe the transient currents were reasonable.

If the inactivation pathways were removed from either model, the channel would burst with kinetics controlled by α_m and β_m. In particular, the observed open-time constant would be simply the inverse of 2 β_m. The closed-time constant, on the other hand, was measured using the approximation of two-state gating, whereas models 1

and 2 assumed three states in the activation pathway (two closed and one open). Although the exact distribution of closed times for such a three-state model would consist of the sum of two exponentials (and the power spectrum of two Lorentzians), in practice only a single component could be detected using the rate constants of our model and the size data sets to which we had access. It was therefore necessary, in order to compare these two measurements, to calculate the effective rate constant, α_m^*, that would be observed if the closed times of this three-state model were approximated by two states. The value of α_m^* is given by:

$$\alpha_m^* = \alpha_m \cdot P_{C2} \tag{10}$$

where P_{C2} is the probability that a closed channel is in state C2 instead of C1, given here by:

$$P_{C2} = \frac{\alpha_m}{\alpha_m + \frac{\beta_m}{2}} \tag{11}$$

The values that we measured for the opening and closing rates (inverse closed- and open-time constants, respectively) during bursts are compared with those expected from our model in Fig. 8, *A* and *B*. Each open square in Fig. 8 *A* is the

TABLE I

Parameters for Two Models of Na^+ Channel Kinetics

Parameter	Model 1	Model 2
$\bar{\alpha}_m$	162 s^{-1}	162 s^{-1}
$\bar{\beta}_m$	563 s^{-1}	563 s^{-1}
$\bar{V}_m$	−43 mV	−43 mV
V_{α_m}	7.4 mV	7.4 mV
V_{β_m}	16.1 mV	16.1 mV
$\bar{\beta}_h$	2,334 s^{-1}	1,900 s^{-1}
$\bar{\beta}_z$	800 s^{-1}	295 s^{-1}
$\bar{V}_h$	−31 mV	−31 mV
V_{β_h}	20.2 mV	—
V_{β_z}	—	35 mV

Constants used in Eqs. 2–7 to determine the rates of transition between states of the Na^+ channel. The rates are presented for the two models that were examined. See text for further detail.

estimate of the opening rate for one burst, measured with power spectral analysis. The squares in Fig. 8 *B* are the estimates of the closing rates from the same analyses. The solid lines are the values of α_m^* and $2\beta_m$ derived from the models and fits presented above. Although the complexity of the underlying kinetic processes, the limited amount of data available during single bursts, and the diverse kinetics seen between bursts all limit the precision with which our kinetic measurements can be made, the opening and closing rates during bursts are very close to those predicted from the macroscopic currents. The underlying processes that control the burst and the activation gating might be closely related. If so, then the diverse behaviors of the

bursting channels could be an indication that the channels that give rise to the early currents also have diverse kinetics.

DISCUSSION

We present here a quantitative study of the gating kinetics of bursting Na^+ channels. Our most important results are that the open- and closed-time constants vary markedly from burst to burst, and do so with little or no correlation with each other. The values that a time constant could attain broadly dispersed at all membrane potentials that we studied. The means of these dispersed time constants were close to those expected from the average activation gating of nonbursting Na^+ channels. Our results therefore suggest that normal transient Na^+ currents might result from a kinetically diverse population of Na^+ channels.

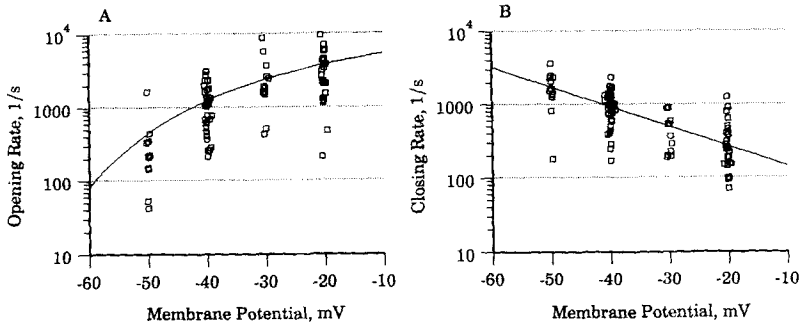

FIGURE 8. The values of the calculated opening (*A*) and closing (*B*) rate constants of the 87 bursts from Fig. 5 are plotted separately as functions of membrane potential for comparison with the opening and closing rates predicted by the models shown in Fig. 6. The solid lines are the values of the apparent opening rate, α_m*, and the closing rate, $2\beta_m$, that would be observed if inactivation were removed from the kinetic scheme discussed in the text.

We thus paint a complex picture of the Na^+ channel: normally, the channel functions in a "mode" in which both activation and inactivation are relatively rapid. After depolarization, the channel opens quickly, then inactivates after one or more brief openings (Aldrich et al., 1983; Horn and Vandenberg, 1984). The rate of a channel's inactivation can occasionally slow, giving rise to prolonged bursts of sequential openings (Patlak and Ortiz, 1986). The kinetics within this bursting "mode" are apparently controlled by the remaining activation/deactivation gates, but, as we have shown, the open-state kinetics differed from one burst to the next (Patlak et al., 1986). The present results, showing broad, uncorrelated dispersion of both the opening and closing rates during bursts further increases the complexity of this kinetic image of the channel. The possible origins of such kinetic diversity are worth considering in depth.

The variability that we observed in the kinetics during bursts was not due to experimental variability. Although most of the bursts that we analyzed were recorded on different patches, the experimental conditions (e.g., solutions, temper-

ature, transmembrane potential, etc.) were nearly identical from one recording to the next. Differences in open- and closed-time constants as large as those reported here would require, for example, variability in transmembrane potential or recording temperature of >10 mV or 10°C. On the other hand, any variability in the early, macroscopic, Na^+ currents from the same patches could generally be explained by differences of just a few millivolts or degrees. Furthermore, variability of the potential or the temperature would have led to measurable correlations between the open and closed times from one recording to the next, which we did not observe.

The kinetic diversity also cannot be explained by the statistical variability introduced by fitting exponential curves to histograms constructed from limited numbers of events. The variability in the best fitting time constants from simulated channel data (performed at similar i/σ and burst lengths) was much smaller than that of our measurements. Even the analysis of 12 sequential bursts from one channel, in which we had no assurance that the channel did not change during the recording, showed much less variability than that between different channels. The use of power spectral analysis, which lowered accuracy and increased variability somewhat, still could not have caused the distribution in values that we observed. Any errors that might have been introduced by our simplifying assumption that the open and closed times could be approximated by single exponentials should have caused a bias of all values in a similar direction, not increase the variability of the measurements. We believe, therefore, that the observed variability is intrinsic to the channels.

Kinetic diversity is also not likely to have been the product of two or more populations of channels, each with its own behavior. If there were populations of channels, each with characteristic kinetic properties, then the measured time constants would fall within two or more discrete areas in plots such as those shown in Figs. 4 and 6. In contrast, the time constants that we observed showed no such tendency to cluster around two or more discrete sets of values, but rather were evenly dispersed in all cases. Furthermore, we saw no indication of multiple classes of open-channel amplitude, which have been used by others to identify discrete channel types (e.g., Weiss and Horn, 1986). The diversity appears, therefore, to be the result of a single type of Na^+ channel.

Diversity within a single population of channels could either be static (fixed permanently at the time of the channel's synthesis or membrane insertion), or dynamic. Our observation that as many as 20% of all bursts showed evidence of kinetic changes during the burst itself (Patlak et al., 1986) points to the latter possibility. This result could, by itself, explain the observation that different members of a channel population, and thus the bursts that they produce, are heterogeneous. If each channel in the membrane changes independently, then with time the population of channels would become randomly distributed in their properties. Our hypothesis of kinetic diversity can thus be expressed as follows: each channel, although on average identical to any other channel, displays diverse, but transient, combinations of transition rates that define its behavior (i. e., "personality") at a given moment. The hypothesis of kinetic diversity, if correct, will have important consequences for our understanding of Na^+ channel function.

Although our observations are consistent with this hypothesis, they give little indication as to the frequency with which Na^+ channels change their properties, nor to

the number of functionally different behaviors that a single channel can express during its lifetime. For example, if an average of 20% of bursts show alterations, then this may indicate that the channel changes its properties every several seconds (5 bursts × 0.4 s per burst). On the other hand, our single observation of a channel that underwent 12 sequential bursts over 120 s with little or no change of its kinetics might indicate a much slower rate of transition. Another alternative is that channels only change kinetics when they are active. Future experiments will be necessary to examine these issues in more depth.

Our hypothesis of kinetic diversity requires no assumptions as to the mechanism involved. The alterations in the channel that give rise to such diverse kinetics might be small variations in the protein conformation, changes in the chemical structure of the channel (extent of glycosylation or phosphorylation for example), the local environment of the channel, or alterations in some pattern of molecular vibration (analogous to harmonics of a tuned system). Whatever the mechanism, the channel's behavior at any moment would be characterized not only by its primary state (e.g., resting, open, and inactivated states of the Na^+ channel), but also by numerous other physical/chemical properties that determine the exact transition rates between the primary states.

Transient changes that lead to the alteration of one or more of a channel's rate constants are usually called "mode" changes (Hess et al., 1984; McManus and Magleby, 1988). For example, reduction of a Na^+ channel's inactivation rate leads to the bursting mode. The inactivation mode change has little or no effect on the activation/deactivation rates, which appear to have independent modes of their own as well. The final behavior of the channel could thus be considered a composite of these multiple kinetic modes.

Whatever the mechanism, the factors that control the "modes" of the channel appear to be long-lived, spanning many hundreds of transitions between the main states. During the interval between kinetic alterations, the channel can be modeled as Markovian, with a small number of states, and constant rates of transition. Modes can be formally incorporated into Markovian models by adding one or more parallel sets of states. Such models, however, require a new set of states for each different combination of rates. Since we see a broad diversity of kinetic behaviors, a large number of very similar modes would be required for a full kinetic description. Such models would be exceedingly complex. It may, in fact, be easier to relax the Markovian assumption of constant transition rates, permitting an individual rate constant to adopt a distributed set of rates.

We believe this is a more reasonable description of the function of a large, complex macromolecule like a channel than standard kinetic models with a small number of states and unique rates of transition. Other large proteins appear to function in a similar manner (see Karplus and McCammon, 1981; Cooper, 1984; Ringe and Petsko, 1985; for reviews). For example, optical studies have shown that the rates of transition between states of the myoglobin molecule are distributed over a range of values (Ansari et al., 1985).

Our observations are significant for the measurement, understanding, and modeling of Na^+ channel behavior. Although the assumption of homogeneity is convenient and appealing in kinetic studies, since it permits easy extrapolation of micro-

scopic results obtained with a small number of measurements to the behavior of the channel population, our results show that such extrapolations need to be made with care. Homogeneity is also an underlying assumption in many statistical tests designed to determine the most appropriate model to describe channel behavior (Aldrich et al., 1983; Horn and Vandenberg, 1984), or to test the independence of channel activity (Kiss and Nagy, 1985). Such studies need to justify further their assumptions and the conclusions derived from them. Finally, dynamic heterogeneity might be a possible explanation for results that are normally attributed either to multiple types of channels, or to additional states added to the basic closed-open-inactivated scheme. Kinetic diversity is an additional complexity that must be accounted for in future studies of channel function.

We thank Drs. W. Gibbons, M. Nelson, C. Patlak, and P. King for helpful comments and discussion.

This work was supported in part by a grant-in-aid from the American Heart Association (AHA 85-0956) and a National Institutes of Health grant (AR-37606). Dr. Patlak is an Established Investigator of the American Heart Association.

REFERENCES

Adrian, R. H., W. K. Chandler, and A. L. Hodgkin. 1970. Voltage clamp experiments in striated muscle fibres. *Journal of Physiology.* 208:607–644.

Aldrich, R. W., D. P. Corey, and C. F. Stevens. 1983. A reinterpretation of mammalian sodium channel gating based on single channel recording. *Nature.* 306:436–411.

Ansari, A., J. Berendzen, S. F. Bowne, H. Frauenfelder, I. E. T. Iben, T. B. Sauke, E. Shyamsunder, and R. D. Young. 1985. Protein states and proteinquakes. *Proceedings of the National Academy of Sciences.* 82:5000–5004.

Attwell, D., I. Cohen, D. Eisner, M. Ohba, and C. Ojeda. 1979. The steady state TTX-sensitive ("window") sodium current in cardiac Purkinje fibres. *Pflügers Archiv.* 379:137–142.

Auerbach, A., and C. J. Lingle. 1986. Heterogeneous kinetic properties of acetylcholine receptor channels in *Xenopus* myocytes. *Journal of Physiology.* 378:119–140.

Bevington, P. R. 1969. Data Reduction and Error Analysis for the Physical Sciences. McGraw Hill Book Co., New York. 119–133.

Blatz, A. L., and K. L. Magleby. 1986. Correcting single channel data for missed events. *Biophysical Journal.* 49:967–980.

Caceci, M. S., and W. P. Cacheris. 1984. Fitting curves to data. *Byte.* 9:340–360.

Campbell, D. T., and B. Hille. 1976. Kinetic and pharmacological properties of the sodium channel of frog skeletal muscle. *Journal of General Physiology.* 67:309–323.

Carmeliet, E. 1984. Slow inactivation of the sodium current in rabbit cardiac Purkinje fibres. *Journal of Physiology.* 353:125P. (Abstr.)

Carmeliet, E. 1987. Slow inactivation of the sodium current in rabbit cardiac Purkinje fibres. *Pflügers Archiv.* 408:18–26.

Colquhoun, D., and A. G. Hawkes. 1977. Relaxation and fluctuations of membrane currents that flow through drug-operated channels. *Proceedings of the Royal Society of London, B.* 199:231–262.

Colquhoun, D., and F. J. Sigworth. 1983. Fitting and statistical analysis of single-channel records. *In* Single Channel Recording. B. Sakmann and E. Neher, editors. Plenum Publishing Corp., New York, London. 191–263.

Conti, F., and E. Wanke. 1975. Channel noise in nerve membranes and lipid bilayers. *Quarterly Reviews of Biophysics.* 4:451–506.

Cooper, A. 1984. Protein fluctuations and the thermodynamic uncertainity principle. *Progress in Biophysics and Molecular Biology.* 44:181–214.

French, R. J., and R. Horn. 1983. Sodium channel gating: models, mimics and modifiers. *Annual Review of Biophysics and Bioengineering.* 12:319–356.

Hamill, O. P., A. Marty, E. Neher, B. Sakmann, and F. J. Sigworth. 1981. Improved patch-clamp techniques for high-resolution current recording from cells and cell-free membrane patches. *Pflügers Archiv.* 391:85–100.

Hamill, O. P., and B. Sakmann. 1981. Multiple conductance states of single acetylcholine receptor channels in embryonic muscle cells. *Nature.* 294:462–464.

Hess, P., J. B. Lansmann, and R. W. Tsien. 1984. Different modes of Ca^{2+} channel gating behavior favoured by dihydropyridine Ca^{2+} agonists and antagonists. *Nature.* 311:538–544.

Hodgkin, A. L., and A. F. Huxley. 1952. A quantitative description of membrane current and its application to conduction and excitation in nerve. *Journal of Physiology.* 117:500–544.

Horn, R., and K. Lange. 1983. Estimating kinetic constants from single channel data. *Biophysical Journal.* 43:207–223.

Horn, R., and C. A. Vandenberg. 1984. Statistical properties of single sodium channels. *Journal of General Physiology.* 84:505–534.

Karplus, M., and J. A. McCammon. 1981. The internal dynamics of globular proteins. *CRC Critical Reviews in Biochemistry.* 9:293–349.

Keller, B. U., R. P. Hartshorne, J. A. Talvenheimo, W. A. Catterall, and M. Montal. 1986. Sodium channels in planar lipid bilayers. Channel gating kinetics of purified sodium channels modified by batrachotoxin. *Journal of General Physiology.* 88:1-23.

Kerry, C. J., K. S. Kits, R. L. Ramsey, M. S. P. Sansom, and P. N. R. Usherwood. 1986. Single-channel kinetics of a glutamate receptor. *Biophysical Journal.* 50:367-374.

Kiss, T., and K. Nagy. 1985. Interaction between sodium channels in mouse neuroblastoma cells. *European Biophysics Journal.* 12:13–18.

McManus, O. B., and K. L. Magleby. 1988. Kinetics states and modes of single large-conductance calcium-activated potassium channels in cultured rat skeletal muscle. *Journal of Physiology.* 402:79–120.

Moczydlowski, E., S. S. Garber, and C. Miller. 1984. Batrachotoxin-activated Na^+ channels in planar lipid bilayers. Competition of tetrodotoxin block by Na^+. *Journal of General Physiology.* 84:665–686.

Neher, E., and B. Sakmann. 1976. Single channel currents recorded from membrane of denervated frog muscle fibers. *Nature.* 260:799–802.

Neher, E., and C. F. Stevens. 1977. Conductance fluctuations an ionic pores in membranes. *Annual Reviews of Biophysics and Bioengineering.* 6:345–381.

Noda M., T. Ikeda, T. Kayano, H. Suzuki, H. Takeshima, M. Kurasaki, H. Takahashi, and S. Numa. 1986. Existence of distinct (sodium channel) messenger RNAs in rat brain. *Nature.* 320:188–192.

Oxford, G. S. 1981. Some kinetic and steady-state properties of sodium channels after removal of inactivation. *Journal of General Physiology.* 77:1–22.

Patlak, J. B. 1984. The information content of single channel data. *In* Membranes, Channels, and Noise. R. S. Eisenberg, M. Frank, and C. F. Stevens, editors. Plenum Publishing Corp., New York. 197–234.

Patlak, J. B. 1988. Sodium channel subconductance levels measured with a new variance-mean analysis. *Journal of General Physiology.* 92:413–430.

Patlak, J. B., K. A. F. Gration, and P. N. R. Usherwood. 1979. Glutamate-activated channels in locust muscle. *Nature.* 287:643–646.

Patlak, J. B., and M. Ortiz. 1986. Two modes of gating during late Na^+ channel currents in frog sartorius muscle. *Journal of General Physiology.* 87:305–326.

Patlak, J. B., M. Ortiz, and R. Horn. 1986. Open time heterogeneity during bursting of sodium channels in frog skeletal muscle. *Biophysical Journal.* 49:773–777.

Press, W. H., B. P. Flannery, S. A. Teukolsky, and W. T. Vetterling. 1986. Numerical Recipes: The Art of Scientific Computing. Cambridge Press, New York. 550–560.

Rao, C. R. 1973. Linear Statistical Inference and Its Applications. John Wiley and Sons, New York. 625 pp.

Reuter, H. 1968. Slow inactivation of currents in cardiac Purkinje fibres. *Journal of Physiology.* 197:233–253.

Ringe, D., and G. A. Petsko. 1985. Mapping protein dynamics by X-ray diffraction. *Progress in Biophysics and Molecular Biology.* 45:197–235.

Sherman, S. J., and W. A. Catterall. 1985. The developmental regulation of TTX-sensitive sodium channels in rat skeletal muscle in vivo and in vitro. *In* Regulation and Development of Membrane Transport Processes. J. S. Graves, editor. John Wiley and Sons, New York 237–265.

Shoukimas, J. J., and R. J. French. 1980. Incomplete inactivation of sodium currents in nonperfused squid axon. *Biophysical Journal.* 32:857–862.

Shrier, A., and E. Cooper. 1987. Inactivation of A-channels in neonatal rat nodose neurons. *Biophysical Journal.* 51:366*a*. (Abstr.)

Sigworth, F. J. 1985. Open channel noise. I. Noise in acetylcholine receptor currents suggests conformational fluctuations. *Biophysical Journal.* 47:709–720.

Sigworth, F. J., and E. Neher. 1980. Single Na channel currents observed in cultured rat muscle cells. *Nature.* 287:447–449.

Vandenberg, C. A., and R. Horn. 1984. Inactivation viewed through single sodium channels. *Journal of General Physiology.* 84:535–564.

Weiss, L. B., W. N. Green, and O. S. Anderson. 1984. Single-channel studies on the gating of batrachotoxin (BTX)-modified sodium channels in lipid bilayers. *Biophysical Journal.* 45:67*a*. (Abstr.)

Weiss, R. E., and R. Horn. 1986. Single-channel studies of TTX-sensitive and TTX-resistant sodium channels in developing rat muscle reveal different open channel properties. *Annals of the New York Academy of Sciences.* 479:152–161.